



NATIONAL ADVISORY COMMITTEE FOR AERONAUTICS

TECHNICAL NOTE NO. 1471EXPERIMENTAL INVESTIGATION OF VELOCITY DISTRIBUTIONS
DOWNSTREAM OF SINGLE DUCT BENDS

By John R. Weske

SUMMARY

Velocity distributions at the outlet of a large number of duct elbows of round and elliptical as well as square and rectangular cross section were measured at Reynolds numbers from 0.2 to 0.6×10^6 and the results presented in tabular form. Special investigations include measurements of the decay of velocity patterns produced by curved ducts and of the effect of asymmetrical upstream velocity distributions. Several techniques of measurement were applied since it was found that there are three distinctive regions of flow in curved ducts, each requiring a particular method of measurement.

The results indicate that velocity distributions in curved ducts of different cross-sectional shape and aspect ratio are quite similar and that the shape and proportions of the duct section are a minor factor compared with radius ratio in regard to their effect upon the velocity pattern. Spiralling motion occurs as a result of upstream velocity distribution asymmetrical with respect to the plane of curvature; double-spiralling motion is encountered downstream of bends of small radius ratio. Both types of motion persist downstream of the curved ducts longer than simple velocity discontinuities. Neither variation of Reynolds number within the range of the tests nor simulated poor matching of duct joints has an appreciable effect upon the velocity distribution in curved ducts.

INTRODUCTION

The velocity distribution in curved ducts has been investigated experimentally, notably by Keulegan and Beij (reference 1) and by Eustice (reference 2). The subject is also treated incidentally in numerous investigations of the pressure loss in curved ducts. The available material, however, is neither comprehensive nor does it apply to the types of duct bend found in aircraft installations nor to the range of Reynolds number encountered in their operation.



For this reason a program of experimental investigation of velocity distributions in curved ducts was undertaken with a twofold objective, namely, for the purpose of providing the designer of aircraft ducting with a substantial body of engineering data relative to the velocity distribution in curved ducts and furthermore for the purpose of identifying the basic factors affecting the velocity distribution. This analysis, it was hoped, might establish a basis from which velocity distributions in curved ducts other than those tested might be predicted with reasonable accuracy.

The project was carried out at the aerodynamics laboratory of the Case School of Applied Science under the sponsorship and with the financial assistance of the National Advisory Committee for Aeronautics. The experimental work and the calculations were performed by Mr. J. Chvosta and Mrs. F. Scott Rodgers, research assistants at the Case School of Applied Science.

SYMBOLS

V	axial velocity component, feet per second
V_m	mean velocity $\left(\frac{\text{Quantity of flow}}{\text{Area of cross section}} \right)$, feet per second
V_t	tangential velocity component in transverse plane of ducts of circular cross section, normal to radius of cross section, feet per second
q	velocity pressure of mean velocity $\left(\frac{\rho V_m^2}{2} \right)$, pounds per square foot
p	static pressure, pounds per square foot
H	total pressure, pounds per square foot
r	mean radius of curvature of curved duct
b_1	width of duct in plane of curvature
b_2	width of duct normal to plane of curvature
V_1, V_2, V_3	velocities defined by figure 13
e_1, e_2, e_3	distances defined by figure 13

D	equivalent diameter $\left(\frac{4 \times \text{Area of duct}}{\text{Length of perimeter}} \right)$, feet
R	Reynolds number $\left(\frac{\rho D V_m}{\mu} \right)$
ρ	mass density, pound-seconds ² per foot ⁴
μ	absolute viscosity, pound-seconds per square foot
r/b_1	radius ratio of curved duct

TEST STAND AND TEST SPECIMENS

Test Setup

The layout of the test stand is shown in figure 1. The centrifugal blower, rated at 5800 cubic feet per minute against a total pressure of 20 ounces per square inch at 3500 rpm, was driven by a direct-current motor connected in a Ward Leonard circuit to a motor generator set. This afforded speed control of great accuracy over a wide range of Reynolds number. For a 6-inch-diameter duct, for instance, it was possible to attain Reynolds numbers of 1,000,000 and to operate at airspeeds through the duct from 25 feet per second to 350 feet per second. Mach numbers were as high as 0.3.

The test setup for tests of ducting on the discharge side of the blower is shown in figure 1 by solid lines, the arrangement for tests on the intake side, by dashed lines. In the former case an intake box of cross section of 36 inches by 36 and length of 48 inches was placed at the blower inlet. The quantity of flow was determined from the pressure drop across four sharp-edged orifices of $4\frac{7}{16}$ -, $7\frac{13}{16}$ -, $6\frac{7}{64}$ -, and $8\frac{7}{8}$ -inch diameter which were arranged symmetrically on a circle in the front wall of this box.

The blower discharged into a plenum chamber of $17\frac{1}{8}$ by $17\frac{1}{8}$ inches in cross section and 48 inches in length in which the air flow was straightened in a honeycomb section of $\frac{3}{4}$ -by $\frac{3}{4}$ -inch cells of 8-inch depth located 24 inches from the blower outlet and by a wire screen of $\frac{1}{100}$ -inch-diameter wire, 18 meshes to the inch, placed 3 inches downstream of the honeycomb. The maximum velocity in the plenum chamber was approximately 30 feet per second. Gradual decrease of area from the plenum chamber to the transition section, the throat of which matched the duct cross section, was accomplished in a fairing section

of 15-inch length. Contraction ratios from the plenum chamber to the duct were approximately 10:1 for the ducts tested.

When testing duct bends on the inlet side, the quantity of flow was measured at the outlet of the plenum chamber by an A.S.M.E. nozzle of $8\frac{3}{4}$ -inch diameter discharging into atmosphere. The ducting was connected to a smaller intake box. The right-angle turn from the ducting into the blower shown in figure 1 was necessary for reasons of available space and necessitated the placing of a set of turning vanes into the box to insure steady operation of the blower at all loads.

Elbows and Ducts

The curved ducts of circular and elliptical cross section tested were carved from solid blocks of laminated wood. The inner surfaces were made very smooth through repeated application of shellac, alternated with sandpapering. Accurate alignment of ducts and elbows within $1/32$ inch was insured by brass dowels inserted into the flanges. The curved ducts of square and rectangular cross section were likewise constructed of wood and treated in the same manner as those of circular cross section.

Straight ducts at the approach and outlet were constructed of galvanized tin in the case of the circular and the elliptic cross section. In order to prevent distortion of the ducts of elliptic cross section, frames were mounted around the ducts at intervals of 12 inches and the ducts were tested under internal pressure, that is, on the discharge side of the blower only. Thereby the correct cross section was maintained within close limits over the entire length of the duct. The straight ducts of square cross section were of wood construction as it was found that the wooden ducts maintained their shape better at higher air pressures than did the metal ducts of square cross-sectional shape. Dimensions of the elbows tested are given in table I.

Equipment for Special Tests

A special inlet bellmouth was constructed for the tests of 6-inch-diameter curved ducts on the inlet side of the blower, as shown in figure 2. This bellmouth was used in the investigations of circulating flow. A lattice of 24 angularly adjustable guide plates served to produce a vortex flow pattern in the duct. A special duct section of 6-inch diameter shown in figure 3, housing a diametral dividing plate with streamlined leading edge and a screen restricting the flow in one of the semicircular passages, was constructed to produce a simple asymmetrical flow pattern.

METHODS OF MEASUREMENT AND MEASURING DEVICES

Velocity distributions in curved ducts were measured by (1) pitot-tube traverses, (2) directional pitot-tube and yaw-head measurements, and (3) hot-wire measurements.

Pitot-Tube Traverses

Pitot-tube traverse measurements in the diametral plane of curvature of the curved ducts were obtained with a rake consisting of 10 total-pressure tubes, 2 static-pressure tubes, and 2 wall taps, as shown in figures 4 and 6 of reference 3. Traverses were also obtained with a pitot-static tube of $\frac{1}{8}$ -inch diameter and standard dimensions, in which case measurements were not restricted as in the case of the rake to points fixed by the location of the tubes.

Directional Measurements

It was found that, except in the diametral plane of curvature, the direction of flow deviated so much from axial that in general pitot-tube measurements from tubes oriented axially were unreliable. Three-dimensional directional measurements with a yaw head were considered but their use was ruled out as it would have doubled or tripled the time required for traverses. It was observed, however, that in the vicinity of the wall, velocity components normal to the wall were small compared with the axial and peripheral components, and two-dimensional directional measurements were found satisfactory.

Tests of a conventional yaw tube of $\frac{1}{4}$ -inch diameter, however, disclosed a considerably large error in its directional reading resulting from static pressure gradient normal to the direction of flow and to the yaw tube, affecting the pressure readings of the lateral holes. It can be shown that a static-pressure gradient normal to the direction of flow of 0.5 velocity pressure per inch, which is not uncommon in curved ducts, produces an error of 2° for a yaw tube of $\frac{1}{4}$ -inch diameter. The obvious remedy, namely, the decrease of the diameter appreciably below $\frac{1}{4}$ inch, was not thought to be feasible as this would unduly decrease the stiffness of the tube. Since static-pressure gradients normal to the direction of flow were found to be large and to occur frequently in the curved ducts, an attempt was made to reduce the error of reading to less than one-half that of the yaw tube by designing the yaw head (fig. 4). The distance between lateral holes was reduced to 0.08 inch as compared with approximately 0.18 inch for the $\frac{1}{4}$ -inch yaw tube. The calibration curve

(fig. 4) indicated that the readings with this tube are sufficiently critical to permit determination of the direction of uniform rectilinear flow with a precision equal to that of the conventional yaw tube. Static-pressure measurements from wall taps were used to supplement directional measurements near the wall.

Hot-Wire Measurements

In an attempt to obtain rapid readings and direct visual observation of the velocity profiles in curved ducts a special traversing device for a hot wire was developed. The hot-wire instrument used with the traversing device has been described in reference 4. This instrument gives readings proportional to the velocity and responds to rapid velocity variations with very small time lag. The directional characteristics of the hot wire are such that it measures only the velocity component in the plane normal to the hot wire. The electrically operated traversing device (fig. 5) oscillated the hot wire along a straight line through a stroke of 6 inches or less, so as to cover the width of the air duct. The frequency of oscillation was 3 cycles per second; hence the maximum speed of the hot wire was approximately 5 feet per second, which is negligible compared with air velocities except in areas of separation. Hot-wire readings by the traversing method were made visible on the screen of a cathode-ray oscilloscope. Deflection of the sweep of the beam proportional to the travel of the hot wire was obtained by a voltage-divider circuit actuated by the traversing device. Records of the traverses were taken either photographically or by tracing the oscilloscope pattern by pencil on transparent paper. A sample oscillograph is shown in figure 6.

The hot-wire measurements were found useful in measuring the velocity profile and the amplitude and wave length of pulsations and in some cases the direction of the flow. A complete directional velocity survey in the area of separation, however, was not undertaken because of the disproportionately large time it was thought to require; this did not seem to be warranted for the purpose in question.

ACCURACY OF MEASUREMENTS

The entire test setup, including the blower, was carefully checked for air leakage. Calibration tests established an accuracy of the measurements of the quantity of flow within ± 1.25 percent. The gages used for pitot-tube and directional measurements were known to be accurate within 1 percent of their range, and in each case gages of a range suitable for the measurement were selected. The inaccuracy of directional measurements referred to previously did not exceed 2°, except in regions of strong fluctuation. Consequently, the circumferential velocities calculated from them may be 10 percent in error, although in general the accuracy is greater.

PROCEDURE OF MEASUREMENTS OF VELOCITY DISTRIBUTION IN CURVED DUCTS

The measurements leading to a velocity survey of a particular duct section consisted of any or all of the following:

1. Total-pressure and static-pressure traverse in the midplane of curvature
2. Directional total- and static-pressure traverse in the midplane normal to the plane of curvature
3. Supplementary directional total- and static-pressure traverses normal to the wall, for example, for ducts of rectangular cross section along lines normal to the plane of curvature and for ducts of circular cross section along various radial lines
4. Supplementary directional boundary-layer traverses for the exploration of secondary flow
5. Exploratory measurements in regions of intense vorticity

CALIBRATION TESTS

Calibration tests to determine upstream conditions when testing curved ducts on the outlet side of the blower were carried out on a 6-inch-diameter straight duct of 14-foot length and consisted in taking rake measurements of velocity traverses in the vertical plane immediately downstream of the inlet to the duct and in a plane 10 feet downstream of the faired transition section. Records of the readings were made by photoprinting the meniscuses of a multitube manometer from which were calculated the nondimensional velocity profiles. Profile (a) in figure 7, taken at the outlet of the transition section, was obtained from a test at $R = 750,000$. The Reynolds numbers for profiles (b) and (c) are 480,000 and 750,000, respectively. These profiles, taken 10 feet or 20 diameters downstream of the transition section, cannot be distinguished from the fully developed profile at the respective Reynolds numbers. On the basis of these results the rule was established of placing a straight duct 20 or more hydraulic diameters in length ahead of the curved ducts, if upstream conditions corresponding to a fully developed boundary layer were desired.

It was observed during these tests that the velocity profiles and the static-pressure distribution across the duct were exceedingly sensitive to angular misalignment of the duct. It appeared that misalignment of the duct caused the portion of the boundary layer near the wall to be displaced toward the side to which the duct was bent, in quite the same manner as in curved ducts. In order to provide against this, ducts were carefully aligned and secured against displacement by reaction forces of the discharge.

RESULTS AND DISCUSSION

The results obtained from the experimental investigation are arranged in the following order: presentation, in detail, of a number of typical velocity-distribution patterns in curved ducts; presentation in tabular form of the principal results from a large number of elbows tested; and presentation of the findings of special investigations undertaken to clarify certain effects encountered in flow through curved ducts.

Typical Distributions

Typical velocity distributions are shown in figures 8 and 9, the former representing the results of measurements at the outlet of a 6-inch-diameter, 90° curved duct of radius ratio $\frac{r}{b_1} = 1.5$ obtained at $R = 0.605 \times 10^6$, the latter, those for a 90° elbow of a $5\frac{5}{16}$ -inch square cross section of $\frac{r}{b_1} = 1.5$ at $R = 0.53 \times 10^6$.

The following features may be pointed out in regard to figure 8. The total pressure plotted nondimensionally as a multiple of the velocity pressure of mean velocity $\frac{H}{q}$ (absolute values of $\frac{H}{q}$ are irrelevant as they depend upon the characteristics of the setup) is essentially constant throughout the main body of the flow, dropping rapidly in the proximity of the inner wall where total-pressure readings fall below the static-pressure readings. Whenever this occurred it was taken as an indication that backflow occurred near the inner wall. No further quantitative significance, however, was attached to pitot-tube readings in the region of eddying flow because of their inherent inaccuracy at the presumably large angles of yaw encountered here.

The nondimensional static pressure $\frac{p}{q}$ rose uniformly from the inner to the outer wall as required by the condition of equilibrium. The velocity in the plane of curvature, rendered nondimensional by dividing through by the mean velocity $\frac{V}{V_m}$ shows a distribution approximating that of the potential flow, that is $V_r = \text{Constant}$, with the exception of a small region near the outside and a much larger region near the inner wall.

In addition to the foregoing results obtained from measurements in the plane of curvature, the results of velocity traverses in the diametral plane normal to the plane of curvature are given in figure 8, namely, the axial velocity profile and the peripheral velocity profile. The former showed a profile similar to that of a straight duct.

The profile of the velocity component parallel to the wall revealed a region of outwardly directed velocities and another region, near the wall, of inwardly directed velocity components. There appears to be a distinct resemblance between the profile of peripheral velocities and of axial velocities, which will be discussed later.

The velocity and pressure survey at the outlet of the elbow of square cross section (fig. 9) reveals in general the same patterns as for the circular section. The total pressure, however, varied considerably along the midplane of curvature; this indicated strong turbulent mixing. The velocity and area of inwardly directed flow parallel to the wall increased from the outside to the inside of the duct. Likewise, the transverse velocity component in the midplane of curvature decreased toward the outer wall from a positive to a negative value.

Results from rake measurements in a number of diametral planes of a 6-inch-diameter, 90° curved duct, with $\frac{r}{b_1} = 0.75$, tested at $R = 0.535 \times 10^6$, are presented isometrically in figure 10. They serve to show that the region of eddying flow extends across the cross-sectional area approximately along a line normal to the plane of curvature. The hump of velocity on either wall is the result of the currents of inwardly directed flow which arise as the part of the boundary layer nearest the wall is displaced toward the inside of the duct. A typical survey of the static-pressure distribution is given in figure 11 for the 90° elbow, with $\frac{r}{b_1} = 0.75$, of circular cross section, at $R = 0.535 \times 10^6$. The curves of nondimensional static pressure $\frac{p}{q}$ along the midplane of curvature and along three other diametral traverses show that static pressures are almost constant along lines normal to the plane of curvature.

Features common to almost all velocity distributions of the duct bends may be noted in figures 8 to 11, where three distinct regions of flow may be distinguished.

The core.— The core is the region in which the flow is predominantly axial, with the radial and peripheral velocity components small, and the deviation of direction of flow from axial is less than the permissible angle of yaw of the pitot tube. The total pressure in this region is fairly constant; the velocity distribution frequently approximates that of potential flow. The static pressure varies but slightly along lines normal to the plane of curvature. As a matter of definition, it appears that as the fully developed velocity profile of a straight duct is disturbed by the curving of the stream, a boundary layer of definite thickness emerges; hence, it seems justified to identify the region here referred to as the "core." This region was surveyed with a pitot tube or rake oriented axially.

The layer of peripheral flow.— The layer of peripheral flow is the region coinciding in general with the region of the boundary layer near the wall, in which the axial velocity component is much less than in the core; the velocity component normal to the wall, so small as to be negligible; and the peripheral velocity component, considerably large. The distribution of static pressure is governed by the static-pressure variation in the core indicated in the preceding paragraph. For convenience, this layer may be thought to extend to the point of the stream where the peripheral velocity is zero, this layer thus covering the entire region of inwardly directed peripheral flow. Measurements in this region were obtained from two-dimensional directional surveys with a pitot and/or a yaw tube inserted normal to the wall.

The region of eddying flow.— The region of eddying flow is the region in which the total pressure is considerably smaller than in the core. Measurements with total-pressure tubes in or near this region must be taken with great caution because of the high probability of errors resulting from yaw. Careful directional measurements near this region have shown in almost every instance that the region of eddying flow was not so large nor so intensely disturbed as had appeared from nondirectional traverses. Distinction must also be made between eddying flow on one hand and separation of flow on the other. The latter, which implies reversal of direction of flow in the region of separation is relatively uncommon in curved ducts, except those of very small radius ratio r/b_1 . The former was encountered in the region adjacent to the inner wall in all curved ducts investigated. The conditions of eddying flow may range from a steady twisting motion to a state of intense random turbulence. It appears that in the absence of backflow the fluid arranges itself in the eddying zone in such manner that the total pressure increases with the distance from the center of curvature of the duct. This was found to be the case especially for duct bends of large radius ratio. Constancy of static pressure along lines normal to the plane of curvature in the core was found to apply also to the region of eddying flow, except that an increase of static pressure near the inner wall was observed as a result of the stagnation region created by the impinging upon each other of the two peripheral currents.

The various specific aspects of flow in curved ducts may be summarized in regard to their qualitative significance with the aid of the schematic presentation (fig. 12). A brief enumeration of these phenomena, which are well known, is given here to facilitate their identification from the measured data; they include:

1. Retardation near the outside wall, acceleration near the inside wall as the fluid enters the curved duct, giving rise to velocities directed toward the inside wall and leading to the establishment of a flow pattern approximating that of constant moment of momentum (station 2).

2. Displacement of the fluid of low axial velocity surrounding the core toward the region near the inside wall and a corresponding outward displacement of the core. The region along the wall in which occur

transverse velocity components parallel to the wall directed toward the inside portion of the duct section has been referred to as the "layer of peripheral flow" (station 3). Two phases of displacement may be distinguished, namely, the initial "shedding" of the portion of the fluid of low velocity which had been accumulated upstream of the curved duct and the subsequent removal of low-velocity fluid as it is produced by the action of skin friction.

3. At the outlet of the curved duct, acceleration of the fluid in the outward portion of the duct area, deceleration in the inward portion, giving rise to transverse velocities directed toward the outside wall.

4. In the straight duct downstream of the curved duct, gradual acceleration of the fluid in the eddying zone and decay of the latter by attenuation of turbulence leading to the reestablishment of an axially symmetrical flow pattern (station 6).

Tabulation of Principal Results

The results of velocity surveys of a large number of duct bends are presented in table I. This table gives the principal dimensions of the duct bends and the Reynolds numbers of the tests. The following significant data were selected to represent the velocity distribution, as indicated in figure 13.

Data from traverse in midplane of curvature.— The boundary-layer thickness of the outside wall is given nondimensionally as e_2/b_1 , where b_1 is the width of the duct in the plane of curvature. Although in fully developed flow in straight ducts the boundary layer extends throughout the cross-sectional area, in curved ducts a distinct layer on the outer wall can be identified and is defined as the region in which velocity decreases rapidly to zero at the wall. The thickness of the region of eddying flow near the inside wall is e_1/b_1 . The nondimensional axial velocity on the center line is V_1/V_m .

In reconstructing the midplane velocity profile from the foregoing data, it may be assumed that the axial velocity throughout the core varies with radius according to the constant-moment-of-momentum relationship $Vr = \text{Constant}$. In the region of eddying flow it may be assumed that in the absence of backflow the axial velocity increases linearly with radius from zero at the inside wall to the value at the common boundary between core and eddy zone.

Data from traverse in midplane normal to plane of curvature.— The thickness of the layer of inwardly directed flow in the midplane normal to the plane of curvature is shown nondimensionally as e_3/b_2 in figure 13,

where b_2 is the width of the duct normal to the plane of curvature.

The maximum velocity of inwardly directed flow $\frac{v_2}{v_m}$ at a distance $\frac{e_3}{b_2}$ from the wall and the radial velocity component on the center line $\frac{v_3}{v_m}$ are also shown in figure 13.

The patterns of velocity components parallel to the radius of curvature of the duct in the midplane normal to the plane of curvature may be reconstructed from these data by plotting a parabola through the three points given, modifying this parabola slightly on the center line to obtain a horizontal tangent, and drawing a straight line from the other end to zero at the wall. A comparison of the data presented in table I reveals a pronounced basic similarity of the various velocity profiles in spite of a considerable random variation of corresponding individual quantities. No striking differences have been encountered, while a survey of the measured data appears to disclose several factors which tend to render the velocity patterns of duct bends of different proportions more uniform than might be anticipated.

The distortion of the velocity pattern is the more pronounced the smaller the radius ratio, particularly for a radius ratio less than 1.0, as would be expected (cf. table I, items 11, 14, and 17). The evidence is not conclusive as to the merits of large radius ratios in this respect (cf. items 7 and 10, 47 and 53). Distortion is small for angles of bend of 30° and less, but large distortions take place between 30° and 90° . Further increase of the angle of bend, however, has relatively slight effect (cf. items 36 to 41 and 45 to 50; exceptions, items 30 to 35).

Backflow along the inside wall in general did not occur in curved ducts of 30° angle of bend (cf. items 5, 8, 21, 25, etc.; exceptions, items 12 and 15). The occurrence of backflow is favored by small radius ratio and by large angle of bend. In addition, increase of aspect ratio b_2/b_1 , when the major axis is normal to plane of curvature, favors the occurrence of backflow (cf. items 8 to 10, 15 to 17, 31 to 33, and 37 to 39). In square sections backflow does not develop as readily as in circular sections (cf. items 6 and 7 and 27 and 28). This, it appears, may be traced to the ready influx of fluid of relatively low total energy into the area along the inside wall, whether it is from the inside corners of the duct sections, in the case of square or rectangular sections, or from the region along the lateral contours of the section. This influx apparently carries sufficient momentum to counteract or at least confine a reversal of flow. These effects of aspect ratio and of the shape of the section are of general significance and permit the conclusion that the shape and proportions of the duct section must be regarded as a minor factor in regard to their influence upon the distortion of the flow pattern in curved ducts.

Special Investigations

Results of special investigations include the decay of the velocity pattern produced by a curved duct in a downstream straight duct and the effect of variations of the upstream velocity profile upon flow in curved ducts.

For practical purposes it appears of interest to know the way and the rapidity with which a particular velocity pattern produced by a curved duct changes with distance downstream of the elbow. Various velocity patterns produced by elbows were analyzed in regard to their characteristics and it was found that these patterns may be considered to be composed of two types of flow pattern, namely, velocity discontinuities and axial vortex filaments. Consequently the decay of a velocity discontinuity and of a single vortex in a circular duct were investigated separately.

Decay of velocity discontinuity.— Velocity traverses were taken in a straight duct of 6-inch diameter at various distances downstream of the special section (fig. 3). The Reynolds number of these tests, based on the mean velocity and the diameter of the duct, was 0.35×10^6 . The velocity profiles on the midplane normal to the dividing wall are shown in figure 14. Curve (a) refers to the traverse at the trailing edge. Further velocity traverses were taken in several cross-sectional planes at various distances downstream of this section, traverses (b), (c), and (d), as indicated. The velocity profiles indicate the rate of decay of the velocity discontinuity; a velocity profile roughly resembling the fully developed profile of a straight duct was reestablished 24.7 diameters downstream of the trailing edge.

Decay of vortex in straight duct of circular cross section.— This series of tests was conducted in a 6-inch-diameter straight circular duct on the inlet side of the blower in which an axial vortex was produced by the special inlet shown in figure 2. Directional total- and static-pressure traverses were obtained along a diameter at various distances downstream of the elbow at $R = 0.304 \times 10^6$ and at a 32.5° setting of the deflecting vanes. From these measurements were calculated the profiles of circumferential velocities, namely, for a distance of 0.7 diameter (curve (a) in fig. 15), for a distance 8.7 diameters (curve (b)), and for a distance 24 diameters (curve (c)). Also shown in this figure are corresponding total-pressure profiles to supplement the evidence from the velocity profiles. It is seen that the vortex decays very gradually from its center, the vortex being quite distinct 24 diameters downstream of its origin. Thus it may be concluded that in elbows which develop a distinct vortex flow, the downstream effect will be felt over a considerably large distance.

Decay of a pattern produced by a 90° elbow.— Velocity-distribution measurements obtained in the midplane of curvature at various distances [downstream of a 90° elbow of circular cross section, 6 inches in diameter,

with radius ratio of 1.5, tested at $R = 0.304 \times 10^6$, are shown in figure 16, namely, the nondimensional velocity profiles and the nondimensional static pressure. The curves indicate that at a distance of 12.3 diameters from the outlet of the elbow, the velocity pattern corresponds fairly closely to a fully developed pattern in a straight duct, whereas as close as 8.3 diameters downstream, the deviations may be considered of minor order. Static pressures in both cases are uniform across the diameter. Of interest is the comparison of the velocity pattern at the outlet and at 2 diameters downstream of the outlet (curves (a) and (b), respectively), which seems to indicate that the main mass of the fluid, performing a motion of two spirals symmetric with respect to the plane of curvature, is displaced toward either side, the region near the plane of curvature being occupied by eddying fluid surging up from the region of the inside wall of the duct. This phenomenon, while difficult to trace by means of measurements, appears to be quite common in ducts of circular cross section and small radius ratio. In this respect the static-pressure distribution 2 diameters downstream of the elbow (curve (b) of fig. 16) is of interest as it indicates an impinging of the fluid upon the inner wall. A similar cyclic variation of the flow in curved ducts has been commented upon by Eustice (reference 2).

Effect of Upstream Conditions.-- Two instances of symmetrical variations of the upstream velocity profile were investigated, namely, variations of the velocity profile such as occur in the approach length of a straight pipe and effect of poorly fitted duct flanges. In addition one condition of asymmetrical variation of the upstream velocity profile was investigated.

The effect of variation of the upstream velocity was investigated by two tests in which a 90° elbow of 6-inch-diameter circular cross section and radius ratio of 1.5 was placed on the discharge side of the blower, first at the end of a straight duct of 10-foot length placed between the plenum chamber and the elbow, then directly against the faired outlet of the plenum chamber without an intervening approach length. In the former case the velocity profile at the inlet of the blower was fully developed; in the latter it was practically flat as seen in curves (b) and (a), respectively, of figure 7. Comparative data from the velocity survey at the outlets of the elbows are given in table I, group 5. Although discernible, the effect of the upstream velocity pattern upon the velocity profile downstream of the elbow is small.

The effect of poorly aligned duct flanges was simulated by soldering a $\frac{1}{8}$ -inch-diameter wire ring circumferentially into the straight duct $\frac{1}{2}$ inch upstream of the inlet of a 90° elbow of 6-inch-diameter circular cross section and radius ratio of 1.5. This elbow was placed on the inlet side of the blower at an approach length of 2 feet. The tests were conducted at a Reynolds number of 0.3×10^6 . Measurements

of the velocity profile in the midplane of curvature 4 inches downstream of the elbow and boundary-layer traverses show an increase of the area of eddying flow as compared with the test of the elbow without ring at corresponding conditions. Likewise there was a slight increase of the quantity of inwardly directed flow in the proximity of the wall. Comparative data are shown in table I, group 6.

The effect of asymmetrical variation of upstream velocity profile was investigated as follows. The upstream velocity profile was varied by placing the duct section shown in figure 3 at the end of a 10-foot approach length directly upstream of the 6-inch-diameter, 90° elbow, with radius ratio of 1.5. In successive tests, run at $R = 0.3 \times 10^6$, the screened section was placed in the inner half of the duct area, the outer half of the duct area, and on one side of the plane of curvature. The resultant flow patterns at the outlet of the duct were determined from numerous pressure and velocity surveys - directional when required - taken in the straight duct at various diameters and distances downstream of the elbow, of which a few typical profiles are shown in figure 17. The test with the screened section placed in front of the inner half of the elbow area produced the profile of axial velocities in the plane of curvature at the outlet of the elbow (curve (a)). This profile is of a type similar to the profile produced by the same elbow with axially symmetrical flow at the inlet (curve (b), replotted from fig. 8), and consequently the effect of the upstream pattern is slight in this case. When placing the screened section in front of the outer half of the elbow area, it might be expected that the region of low velocities might persist throughout the bend in the outer portion of the area where it was produced; likewise the region of high velocities might remain in the inner portion. Thus the resulting velocity profile at the outlet might have a shape roughly antisymmetric to the profile curve (a) with respect to the axis of the duct. Contrary to this expectation, however, the profile at the outlet of the bend (curve (c)) shows high velocities in the outside portion, being similar to curves (a) and (b). This proves that a nearly complete interchange of the low and high velocity regions had taken place in the elbow.

Results of tests with the screened section on either side of the plane of curvature indicated axial velocity profiles of which curves (d) and (e) of figure 17 are typical. In addition, nondimensional static pressures and tangential velocities in the plane of curvature are included. These curves are evidence of a pronounced rotary motion such that the fluid of higher velocity which had passed through the nonscreened section spirals in the duct, appearing in successive traverses first on one side and then on the other of the duct until the fluid of higher kinetic energy is rather uniformly distributed around the circumference and surrounding the fluid of lower kinetic energy. The results obtained from the foregoing series of tests are believed to give an indication of the velocity distribution to be expected from the combination of two 90° elbows in a 180° bend, in a Z-bend, and in a 90° offset three-dimensional bend.

CONCLUSIONS

Experimental investigation of velocity distributions downstream of single duct bends has led to the following conclusions:

1. Several distinctive regions of flow may be defined in curved ducts operating at high Reynolds numbers, referred to as the "core," the "layer of peripheral flow," and the "region of eddying flow." The characteristics of flow in each region must be taken into account and special methods of measurement applicable in each region must be employed when surveying the flow pattern.
2. The foremost factor affecting the flow at high Reynolds numbers in curved ducts is the displacement of fluid of relatively lower total energy toward the region near the inside wall of the curved duct. This motion and the corresponding outward displacement of the core account for the more important features of velocity profiles in curved ducts.
3. While a region of eddying flow near the inside wall of curved ducts is encountered as a result of displacement flow in all cases, separation of flow accompanied by reversal of flow occurs only in a minority of curved ducts, particularly those of more than 30° angle of bend, of small radius ratio, and of large aspect ratio. The shape and proportions of the duct section are a minor factor in regard to their effect upon the distortion of the flow pattern in curved ducts.
4. From measurements of total-pressure variation in curved ducts, it is inferred that instability of flow near the outer wall of duct bends of large aspect ratio leads to mixing of fluids of different kinetic energies. In curved ducts of small aspect ratio this tendency is not as preponderant since the fluid of lower kinetic energy is displaced more readily toward the inside portion of the duct.
5. Pronounced variations of velocity produced by curved ducts decay relatively rapidly in the straight duct downstream of the outlet, whereas spiralling motion persists over a great distance.
6. Spiralling motion concentric with the axis of the duct occurs as the result of upstream patterns asymmetrical with respect to the plane of curvature of the duct. Double-spiralling motion roughly symmetrical with respect to the plane of curvature occurs as the result of violent separation in elbows of small radius ratio. Cyclic variations of the velocity pattern may persist over a distance downstream of the curved duct as a result of a separation of fluid masses of larger total pressure from those of smaller total pressure.
7. The tests, which extended over a range of Reynolds number at a mean value of approximately 400,000, that is, in the region of

well-developed turbulent flow, did not reveal an appreciable effect of variation of Reynolds number upon the velocity profiles.

8. The length of straight-approach duct to the curved duct and the poor matching of duct joints both influence the upstream velocity pattern and have a noticeable though slight effect upon the velocity distribution in curved ducts.



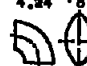
Case School of Applied Science
Cleveland, Ohio
January 13, 1947

REFERENCES

1. Keulegan, Garbis H., and Beij, K. Hilding: Pressure Losses for Fluid Flow in Curved Pipes. Res. Paper 965, Nat. Bur. of Standards Jour. Res., vol. 18, no. 1, Jan. 1937, pp. 89-114.
2. Eustice, J.: Flow of Fluids in Curved Passages. Engineering, vol. 120, 1925, p. 604.
3. Weske, John R.: Pressure Loss in Ducts with Compound Elbows. NACA ARR, Feb., 1943.
4. Weske, John R.: Measurement of the Arithmetic Mean Velocity of a Pulsating Flow of High Velocity by the Hot-Wire Method. NACA TN No. 990, 1946.

TABLE I.- VELOCITY DISTRIBUTION AT OUTLET OF CURVED DUCTS

[A, backflow on inside wall; B, no backflow; C, H constant throughout core; D, H varies throughout core; E, tested at outlet of blower; F, tested at inlet of blower. All items except items 64 to 66 tested with fully developed velocity profile upstream of curved duct.]




Duct bend										Profile in plane of curvature			Profile in midplane normal to plane of curvature			Identification (See fig. 11.)	Item Group				
Cross section	Dimensions of cross section	Straight length (ft)		Area (sq in.)	b_2/b_1	Mean radius of curvature of elbow, r (in.)	Radius ratio, r/b_1	Angle of duct bend (deg)	Reynolds number of tests, R	v_2/b_1	v_1/b_1	V_1/V_m	v_2/b_2	V_2/V_m	V_3/V_m						
		Upstream	Downstream																		
Circular	6-inch diameter 	10	4	28.2	1	4.5	0.75	90	0.15 to 0.81 x 10 ⁶	.02	.33	1.15	.09	-0.18	.07	ADK	1				
						6	1.0	30	-----do-----	.05	.10	1.1	.50	-.25	-.03	BDF	2				
							60	-----do-----	.10	.18	1.1	.30	-.63	.12	BDF	3					
							90	-----do-----	.05 ^a	.15	.99	.27	-.55	.06	ACF	4					
						9	1.5	30	-----do-----	.05	.15	1.09	-----	-----	-----	BDF	5				
							60	-----do-----	.05	.30	1.2	-----	-----	-----	ACF	6					
							90	-----do-----	.05	.30	1.21	.17	-.23	.14	ADP	7					
						24	4.0	30	.53	.02	.15	1.01	.50	-.47	-.07	BDF	8				
							60	-----do-----	.02	.50	1.03	.50	-.43	0	BDF	9					
							90	-----do-----	.02	.40	.90	.50	-.43	-.06	BDF	10					
Elliptical	b_1 (in.) 3.97 b_2 (in.) 10.7  Plane of curvature	7	4	28.2	3	2.65	0.75	90	.44	.02	.40	1.37	.11	-.24	.22	ADK	11				
						5.25	1.5	30	-----do-----	.02	.23	1.09	.06	-.09	.24	ADK	12				
							60	-----do-----	.02	.30	1.12	.11	-.14	.22	ADK	13					
							90	-----do-----	.02	.30	1.1	.13	-.14	.20	ADK	14					
						14	4.0	30	-----do-----	.02	.17	1.06	.04	-.09	.09	ADK	15				
							60	-----do-----	.02	.20	1.08	.07	-.04	.11	ADK	16					
							90	-----do-----	.02	.30	1.06	.07	-.10	.17	ADK	17					
						Elliptical	4.24 	88.1	2	8.45	2.0	30	-----do-----	.02	.16	1.28	.03	-.02	.32	ADK	18
												60	-----do-----	.02	.23	1.24	.04	-.03 ^a	.25	ADK	19
												90	-----do-----	.02	.42	1.32	.06	0	.35	ADK	20

*Values, listed as measured, could not be related to corresponding data for unexplained reasons.



TABLE 1.- VELOCITY DISTRIBUTION AT OUTLET OF CURVED DUCTS - Continued

[A, backflow on inside wall; B, no backflow; C, R constant throughout core;
D, R varies throughout core; E, tested at outlet of blower; F, tested at
inlet of blower. All items except items 64 to 66 tested with fully developed
velocity profile upstream of curved duct]

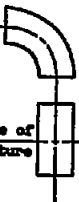

Duct bend										Profile in plane of curvature			Profile in midplane normal to plane of curvature			Identification (See fig. 11.)	Item Group		
Cross section	Dimensions of cross section		Straight length (ft)		Area (sq in.)	b_2/b_1	Mean radius of curvature of elbow, r (in.)	Radius ratio, r/b_1	Angle of duct bend (deg)	Reynolds numbers of tests, R	v_2/b_1	v_1/b_1	V_1/V_R	v_3/b_1	V_2/V_R			V_3/V_R	
			Upstream	Downstream															
Square		5.31	5.31	7	4	28.0	1	3.9	0.75	30	0.15 to 0.53 x 10 ⁶	0.12	0.12	0.10	0.03	-0.06	0.20	BCE	21
										60	-----do-----	.08	.30	1.30	.06	-.25	.30	ACE	22
										90	-----do-----	.03	.35	1.35	.06	-.12	.55	ACE	23
										180	-----do-----	.04	.50 ^a	2.0	0	0	.49	AME	24
								7.75	1.5	30	-----do-----	.10	.12	1.1	.05	-.06	.16	BCE	25
										60	-----do-----	.08	.35	1.13	.09	-.15	.25	BCE	26
										90	-----do-----	.04	.40	1.2	1.04	-.22	.43	BCE	27
										180	-----do-----	.05	.60	1.1	.08	-.12	.17	BCE	28
								20.75	4.0	90	-----do-----	.10	.46	1.1	.19	-.25	.02	BCE	29
								Rectangular major axis perpendicular to plane of curvature	 Plane of curvature	3.07	9.21	7	4	28.0	3	4.6	1.5	30	.43
60	.53	.02	.16	1.0	.03	-.24	.16											ADF	31
90	-----do-----	.03	.16	1.11	.05	-.28	.13											ADF	32
120	-----do-----	.03	.32	1.13	.04	-.61	.40											ADF	33
150	-----do-----	.05	.50	1.09	-----	-----	-----											ADF	34
180	-----do-----	.05	.50	1.08	-----	-----	-----											ADF	35
Rectangular major axis in plane of curvature		9.21	3.07	10	4	28	1 1/2	15.75	1.5	30	.43	.02	.07	1.11	.07	-.14	.19	BCE	36
										60	-----do-----	.02	.22	1.10	.15	-.22	.30	BCE	37
										90	-----do-----	.03	.30	1.06	.15	-.24	.32	BCE	38
										120	-----do-----	.01	.35	.97	.11	-.23	.28	BCE	39
										150	-----do-----	.01	.38	.98	.04	-.03	.22	BCE	40
										180	-----do-----	.02	.44	1.02	.09	-.17	.20	AME	41

^aValues, listed as measured, could not be related to corresponding data for unexplained reasons.

NACA

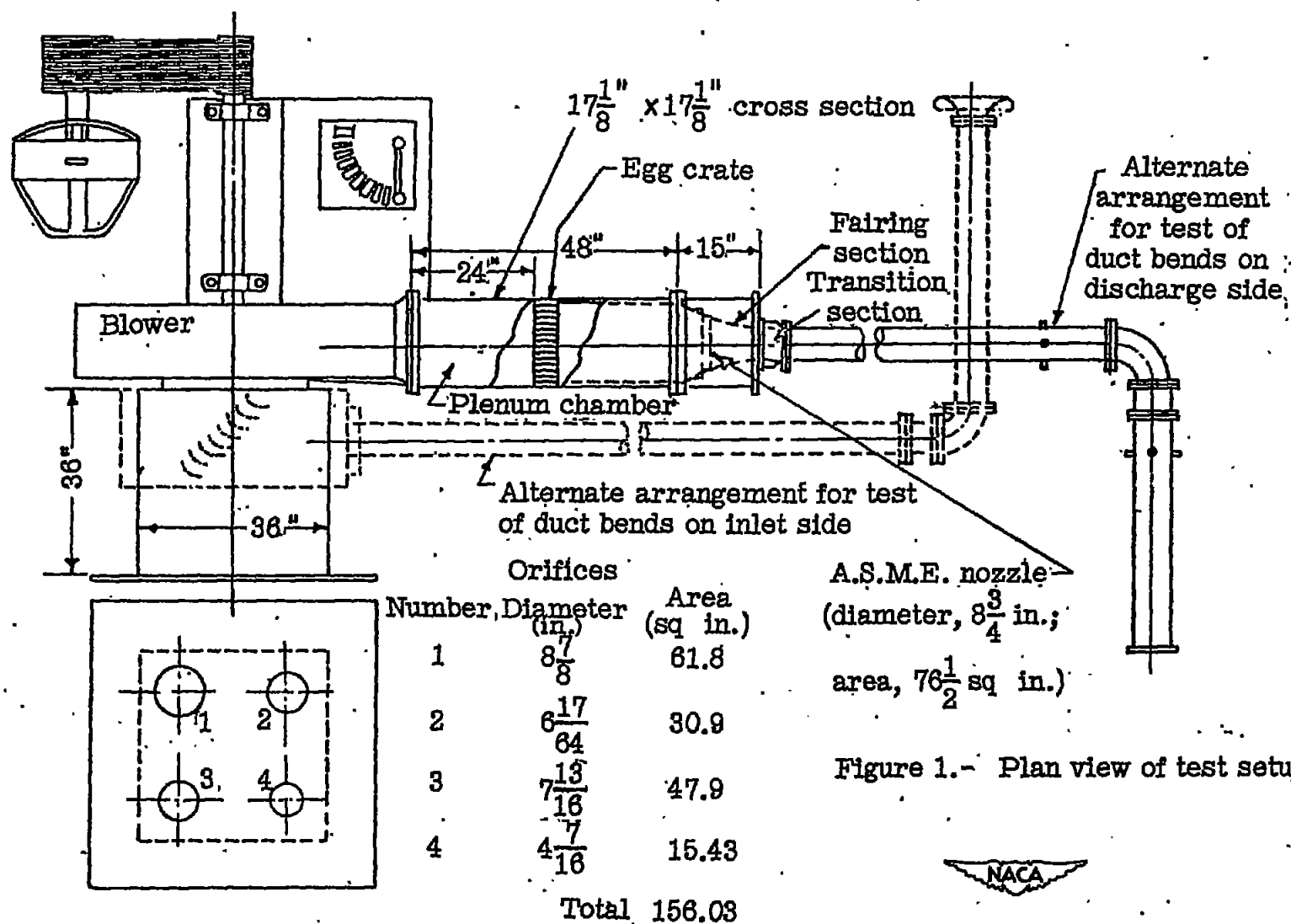
TABLE 1.- VELOCITY DISTRIBUTION AT OUTLET OF CURVED DUCTS - Continued

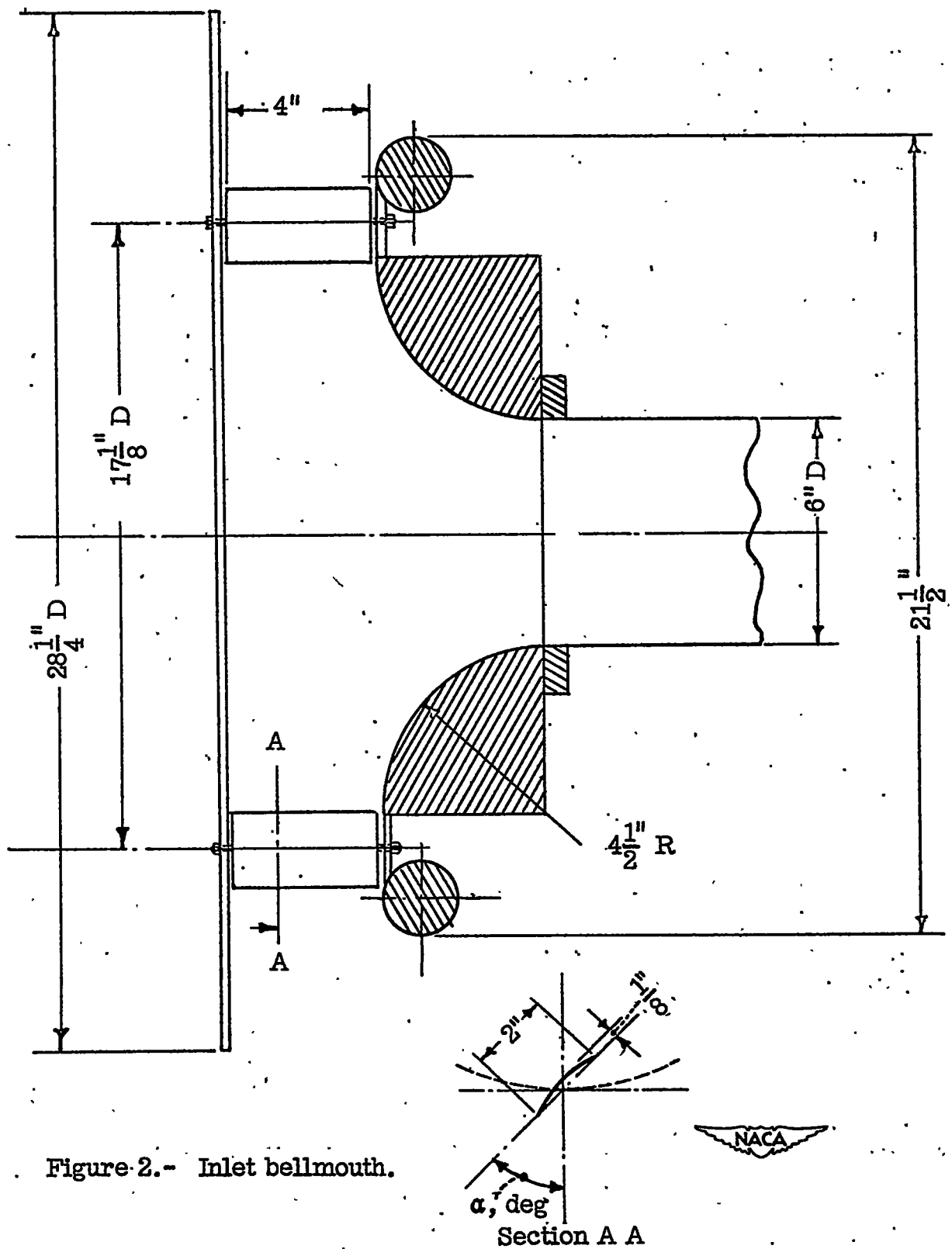
[A, backflow on inside wall; B, no backflow; C, H constant throughout core; D, H varies throughout core; E, tested at outlet of blower; F, tested at inlet of blower. All items except items 64 to 66 tested with fully developed velocity profile upstream of curved duct]

Duct bend											Profile in plane of curvature			Profile in midplane normal to plane of curvature			Identification (See fig. 11.)	Item	Group						
Cross section	Dimensions of cross section	Straight length (ft)		Area (sq in.)	b_2/b_1	Mean radius of curvature of elbow, r (in.)	Radius ratio, r/b_1	Angle of duct bend (deg)	Reynolds numbers of tests, R	e_2/b_1	e_1/b_1	V_1/V_m	e_3/b_2	V_2/V_m	V_3/V_m										
		Upstream	Downstream																						
Rectangular major axis perpendicular to plane of curvature 	3.75 7.52	7	4	28.1	2	3.75	1.0	30	0.47×10^6	0.01	0.21	1.35	0.03	-0.20	0.18	ACE	42	5							
								60	----do----	.01	.30	1.29	.05	-.30	.21	ADE	43								
								90	----do----	.01	.42	1.33	.04	-.36	.15	ADE	44								
						7.5	2.0	30	.52	.01	.16	1.20	.50	-.45	-.15	BDE	45								
								60	----do----	.01	.27	1.19	.50	-.47	-.08	ADE	46								
								90	----do----	.01	.40	1.26	.50	-.56	-.06	ADE	47								
								120	----do----	.01	.35	1.17	.50	-.48	-.13	ADE	48								
								150	----do----	.01	.53	1.10	.07	-.20	.05	ACE	49								
								180	----do----	.01	.66	1.0	.03	-.09	.04	ADE	50								
						15	4.0	30	----do----	.01	.21	1.15	.08	-.20	.10	BDE	51								
								60	----do----	.02	.21	1.14	.05	-.19	.05	BDE	52								
								90	----do----	.02	.27	1.1	.03	-.21	.10	ADE	53								
						Rectangular major axis in plane of curvature 	7.52 3.75	7	4	28.1	0.5	7.5	1.0	30	.47	.01	.08		1.15	.05	-.06	.24	BOE	54	5
														60	----do----	.01	.22		1.19	.08	-.27	.44	ADE	55	
														90	----do----	.01	.33		1.26	.11	-.38	.52	ADE	56	
15	2.0	30	----do----	.01	.20							1.16	.11	-.19	.26	ACE	57								
		60	----do----	.01	.33							1.27	.15	-.29	.31	ACE	58								
		90	----do----	.02	.46							1.22	.17	-.25	.31	ACE	59								
30	4.0	30	----do----	.02	.25							1.24	.09	-.10	.24	BOE	60								
		60	----do----	.02	.46							1.27	.11	-.12	.32	BOE	61								
		90	----do----	.02	.60							.94	.17	-.11	.18	BDE	62								
Circular	6-inch diameter	10	4										1.5	90	.53	.05	.30	1.21	.17	-.23	.14	ADP	63	5	
Circular	6-inch diameter	0	4										1.5	90	.53	.02	.16	1.10	.10	-.12	.05	ADP	64		
Circular	6-inch diameter	2	4										1.5	90	.30	.02	.20	1.15	.10	-.20	.05	ADP	65	6	
Circular	6-inch diameter	2	4										1.5	90	.30	.05	.50	1.22	.20	-.35	.08	BDP	66		

*Values, listed as measured, could not be related to corresponding data for unexplained reasons.

NACA





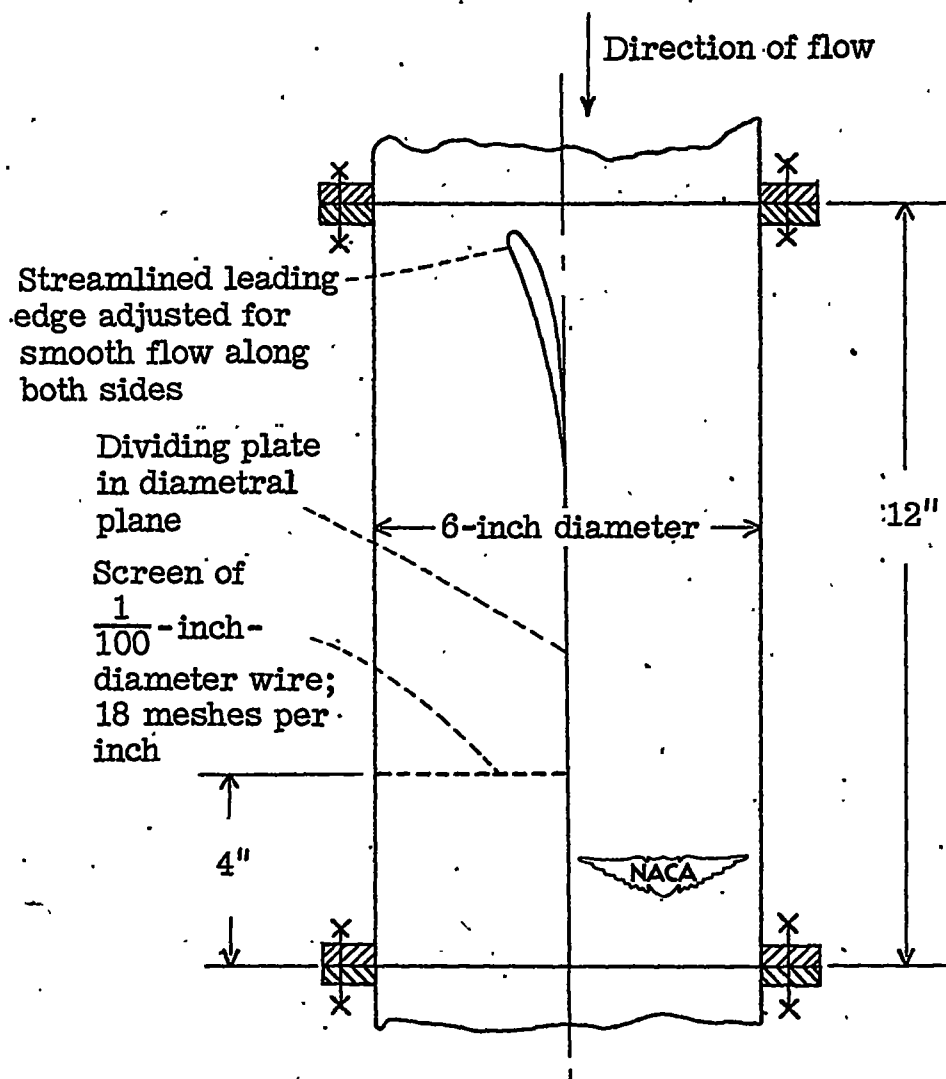


Figure 3.- Half-screened duct section.

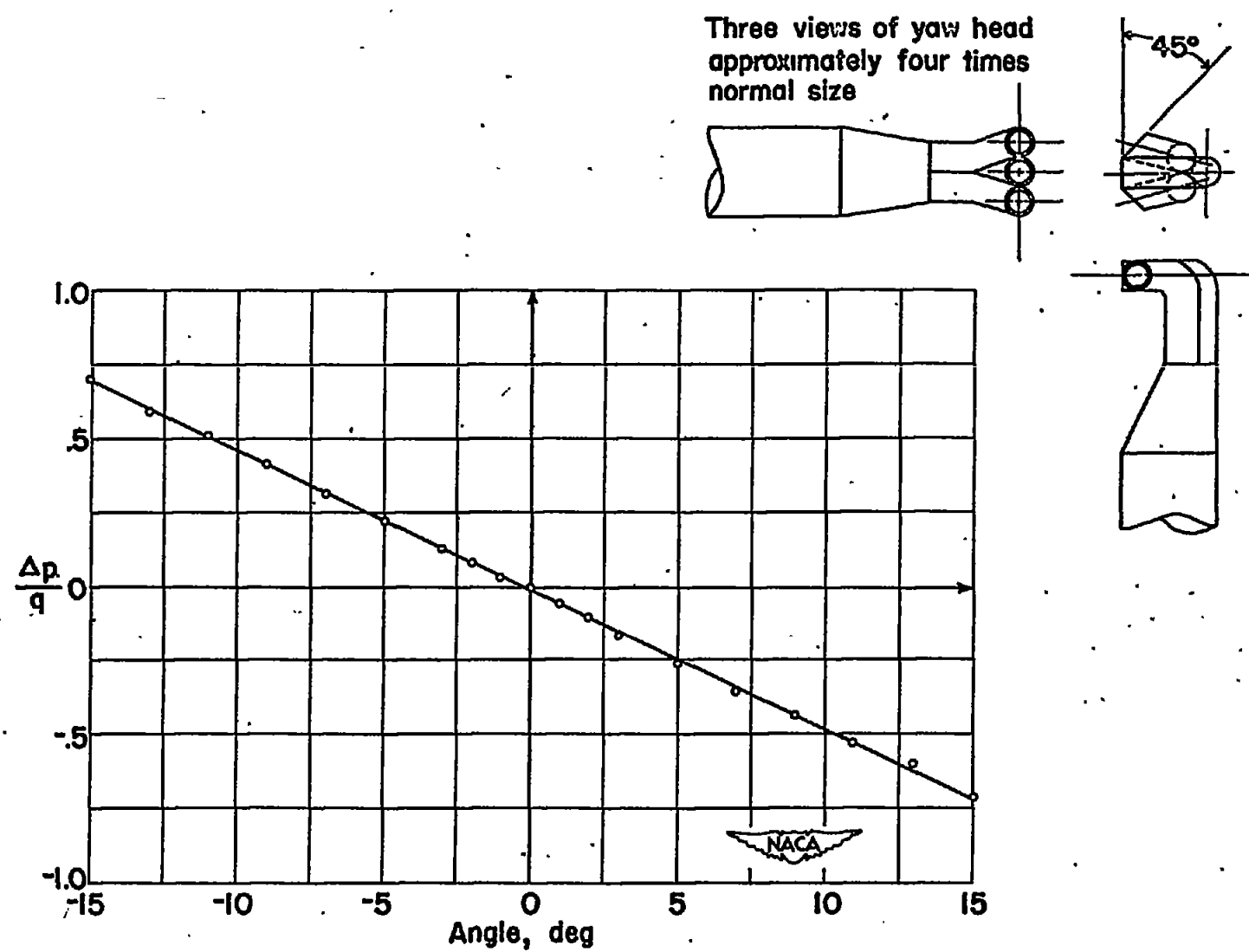


Figure 4.- Yaw-head directional calibration.

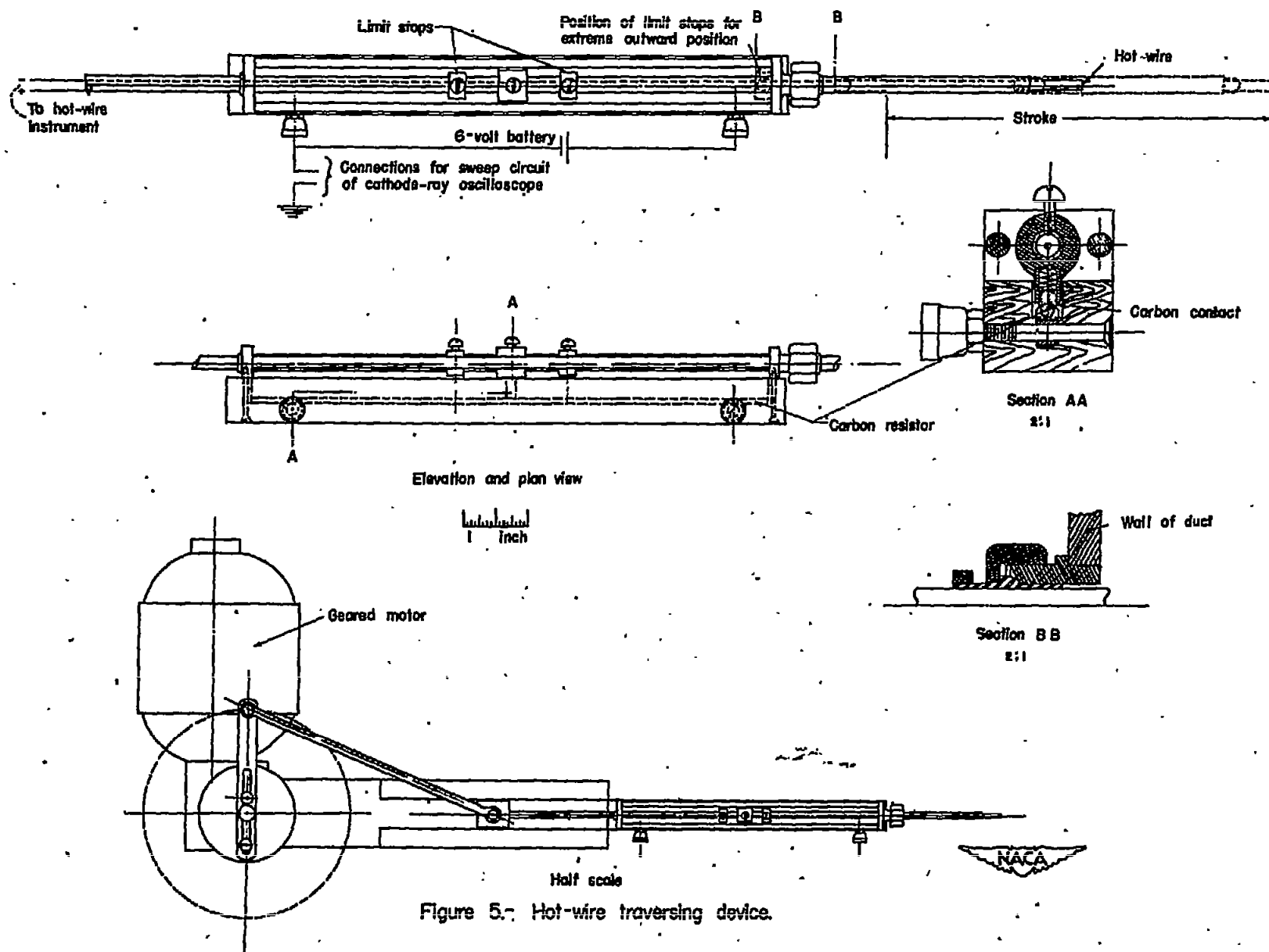


Figure 5.- Hot-wire traversing device.

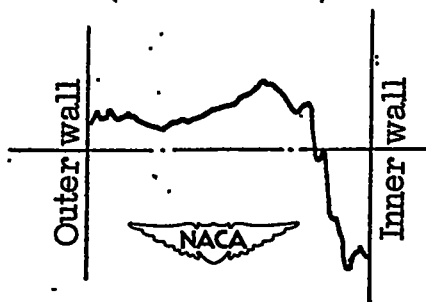
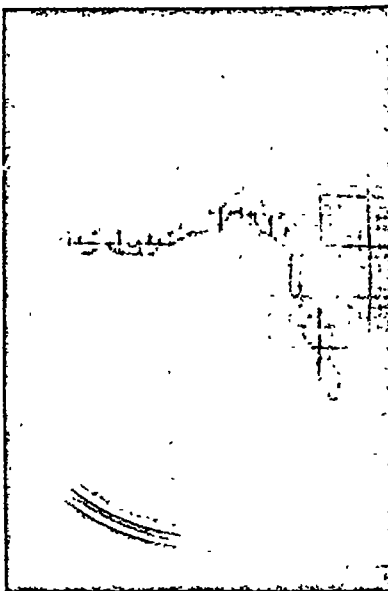


Figure 6.- Oscillograph of velocity traverse.

Note: pg 28 of report was blank
18/11

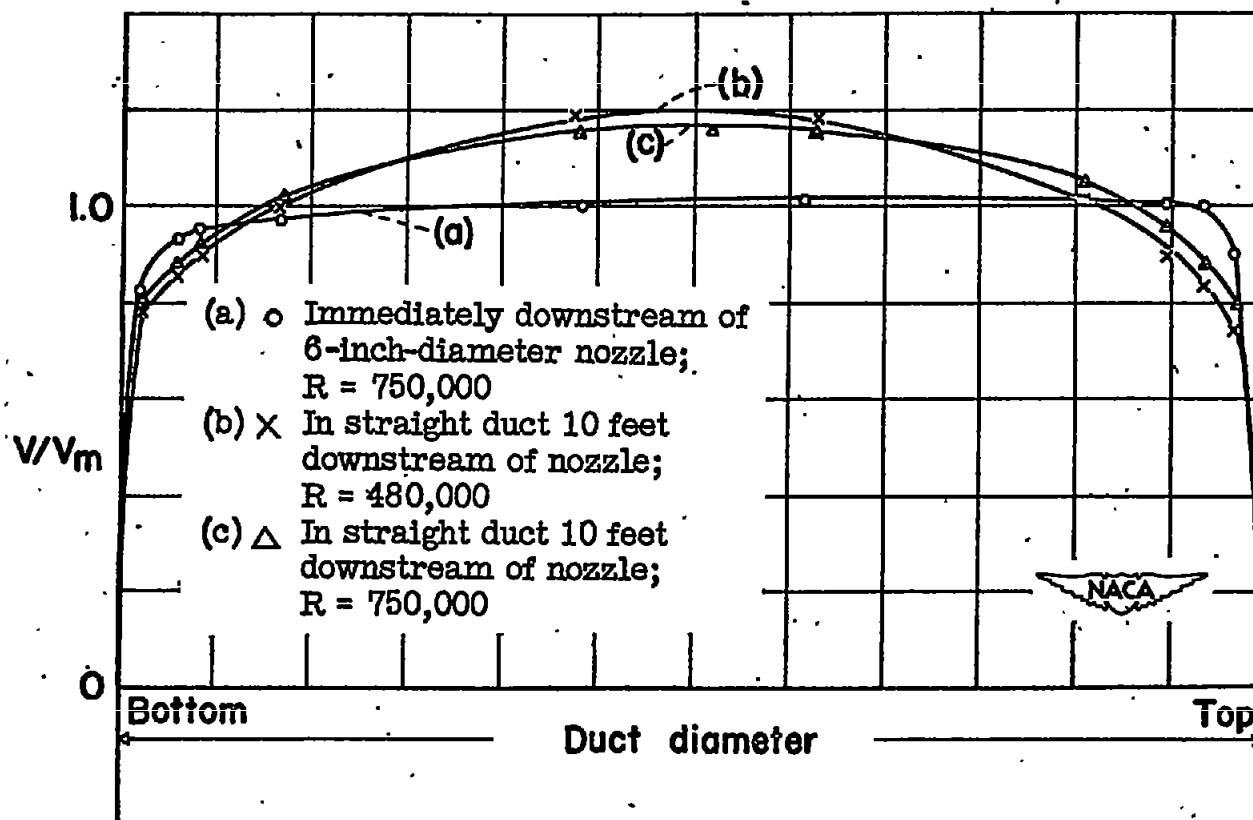


Figure 7.- Nondimensional upstream velocity profiles in circular duct of 6-inch diameter.

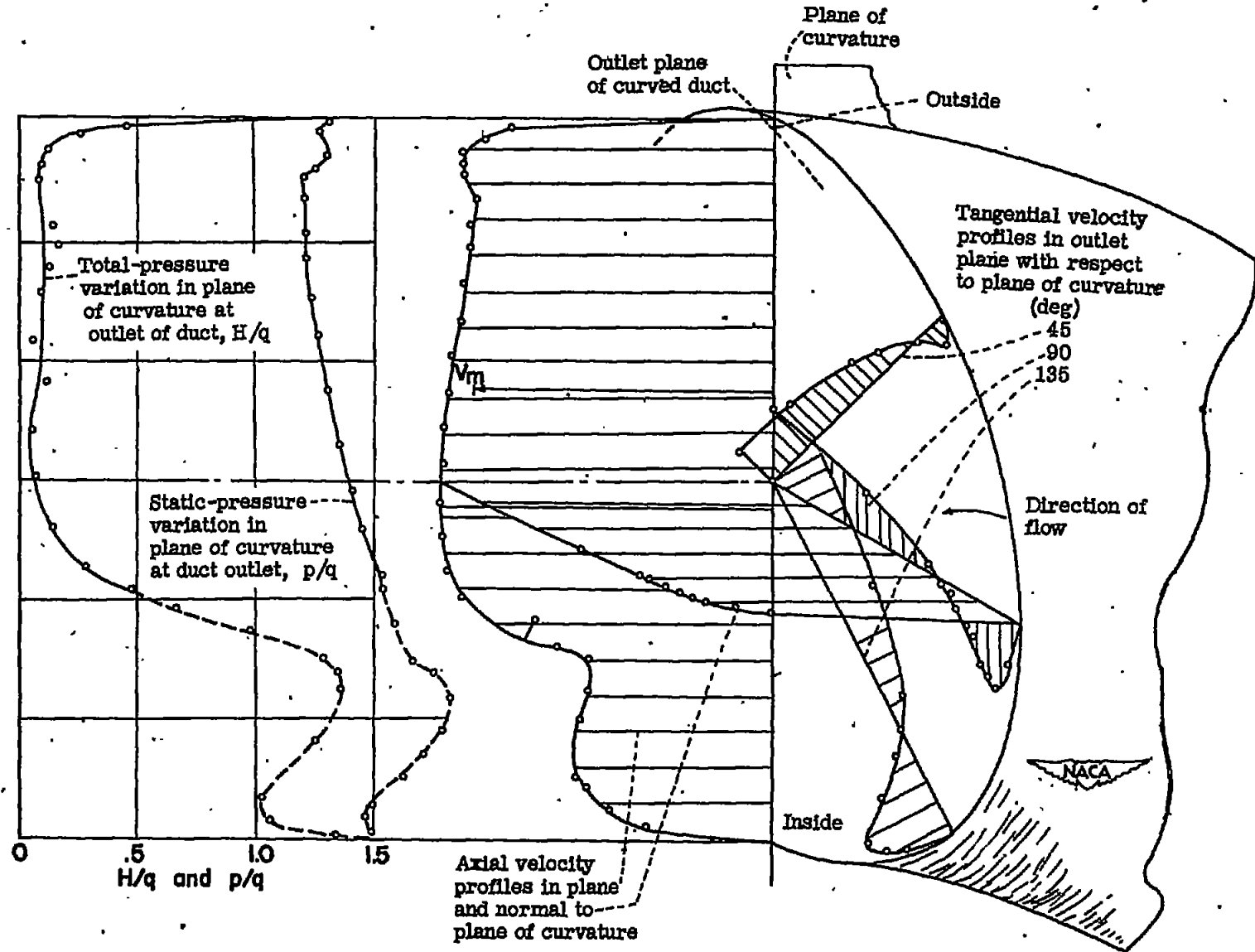


Figure 8.- Velocity distribution at outlet of a 90°, 6-inch-diameter elbow. $\frac{r}{b_1} = 1.5$;
 $R = 0.605 \times 10^6$. Velocities plotted as a fraction of mean velocity V_m .

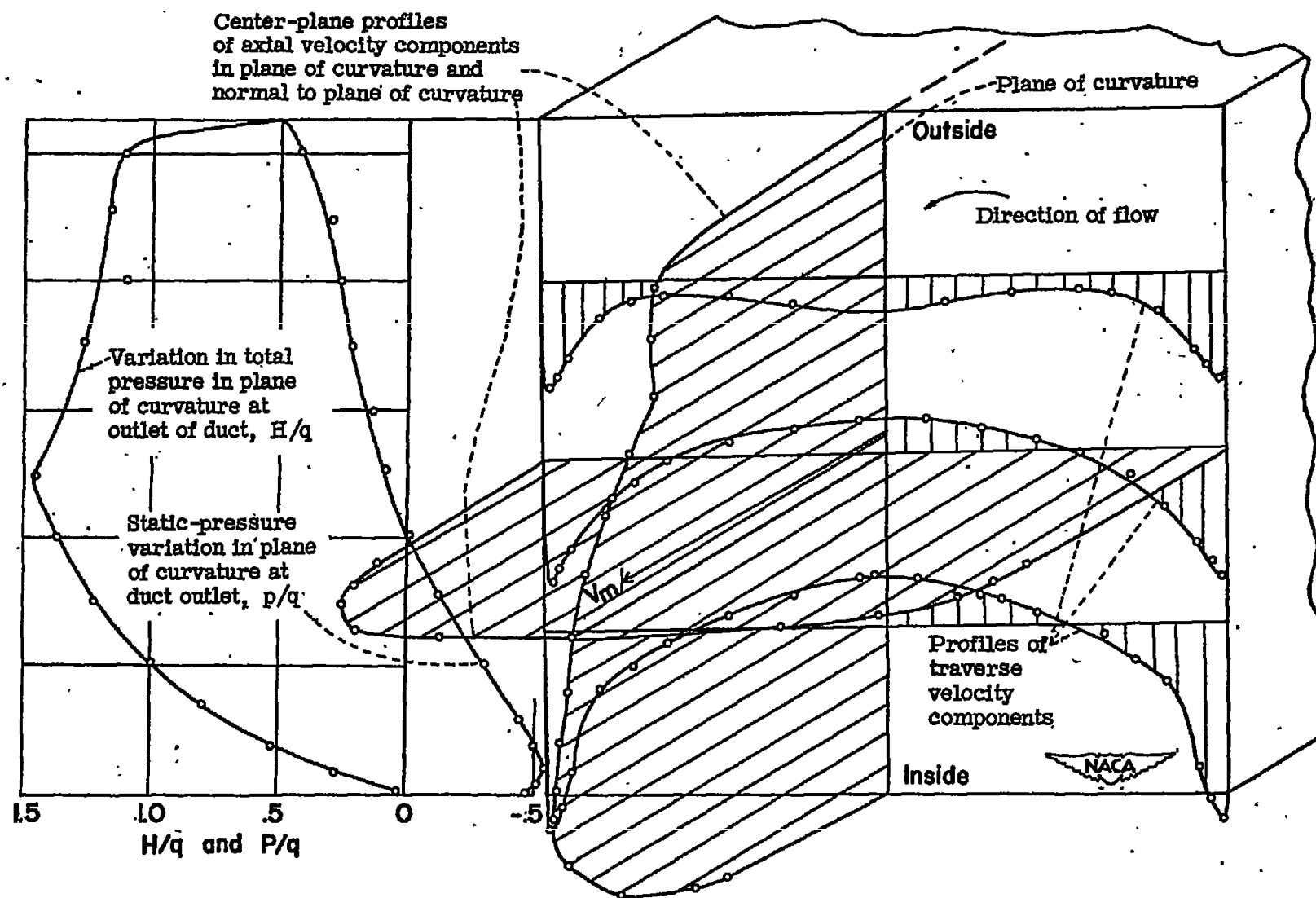


Figure 9.- Velocity survey at the outlet of a 90° elbow. $\frac{r}{b_1} = 1.6$; $5\frac{5}{16}$ by $5\frac{5}{16}$ -inch square cross section; $R = 0.53 \times 10^6$. Velocities plotted as a fraction of mean velocity V_m .

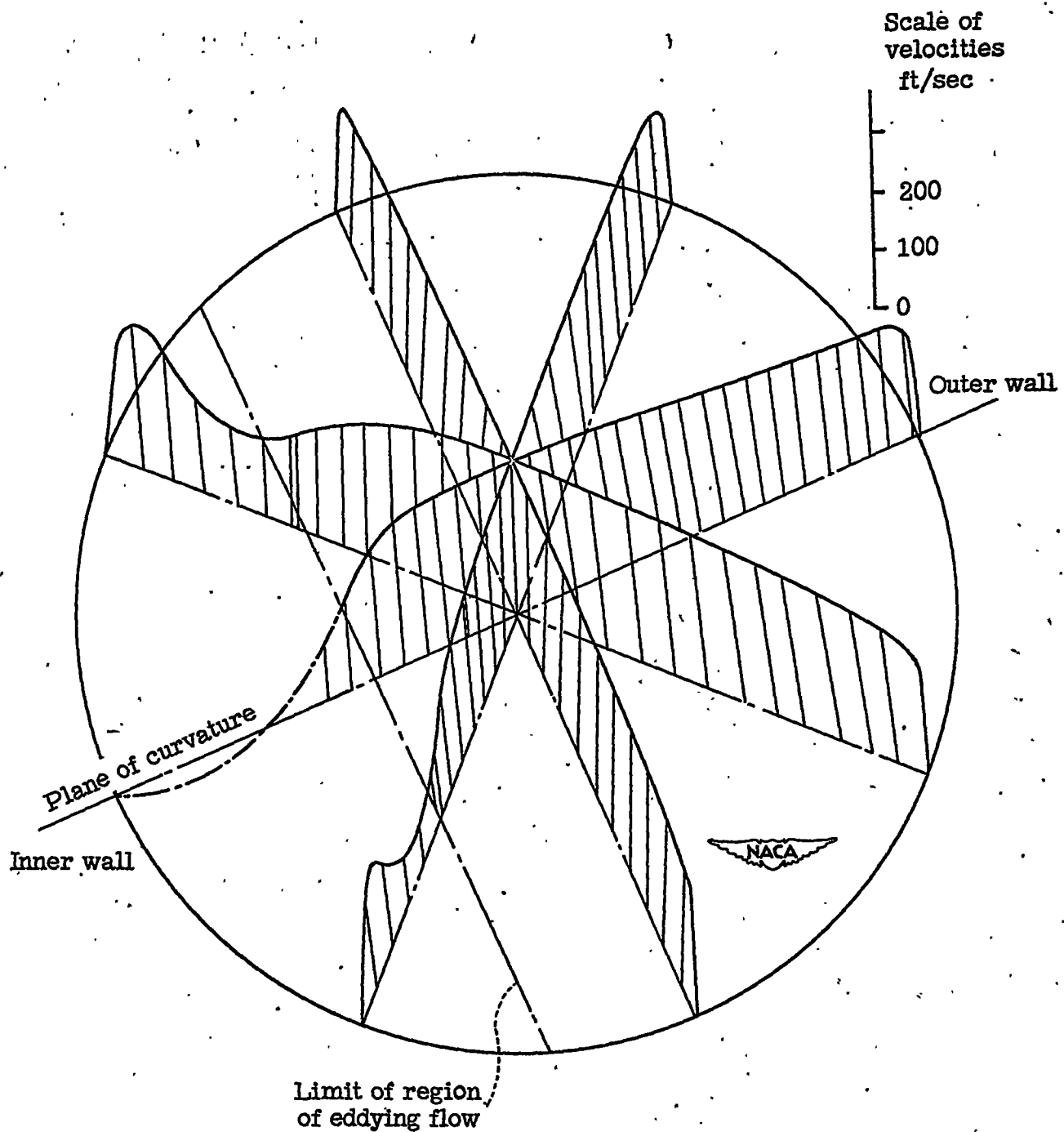


Figure 10.- Velocity distribution at outlet of 6-inch-diameter, 90° elbow. $\frac{r}{b_1} = 0.75$; $R = 0.535 \times 10^6$.

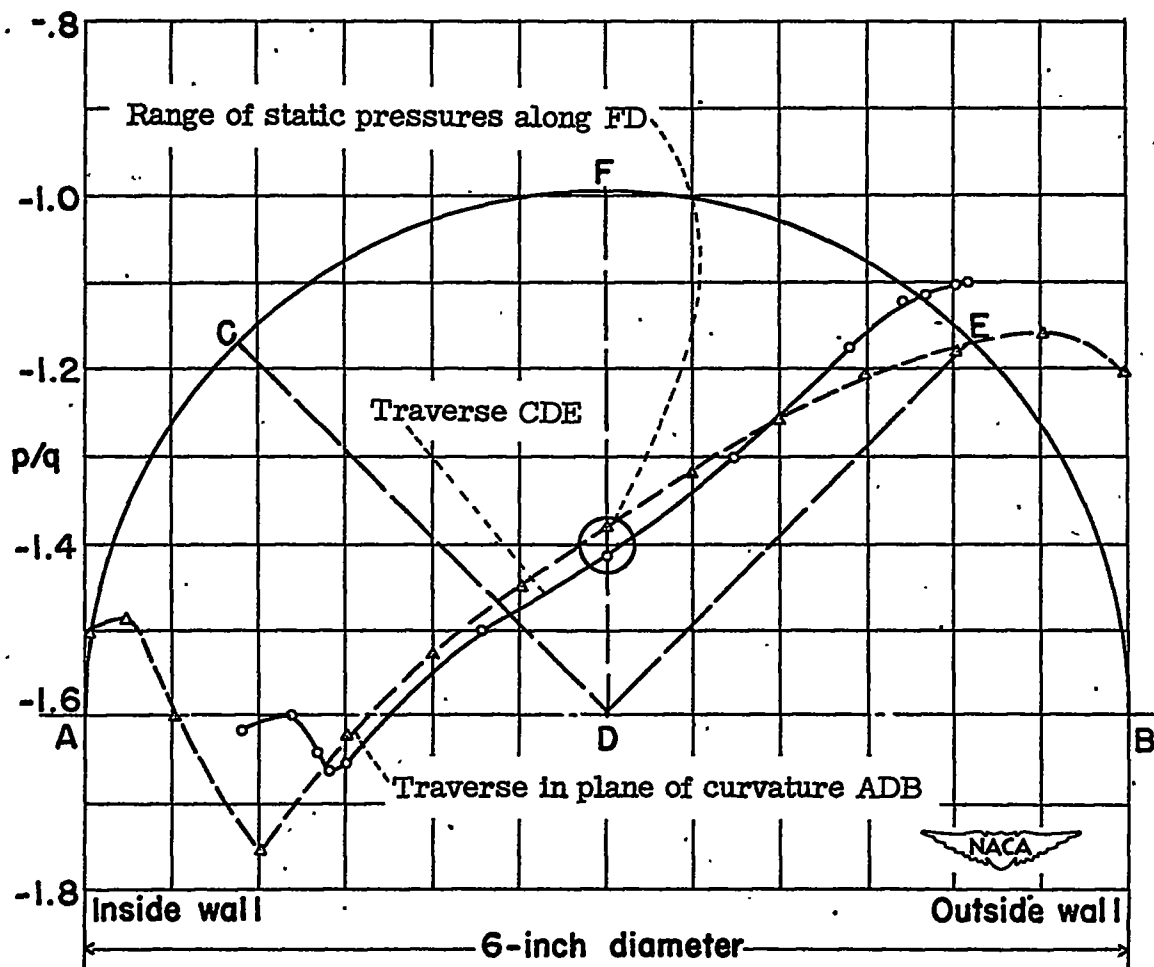


Figure 11.- Static-pressure distribution at outlet of 6-inch-diameter, 90° elbow. $\frac{r}{b_1} = 0.75$; $R = 0.535 \times 10^6$.

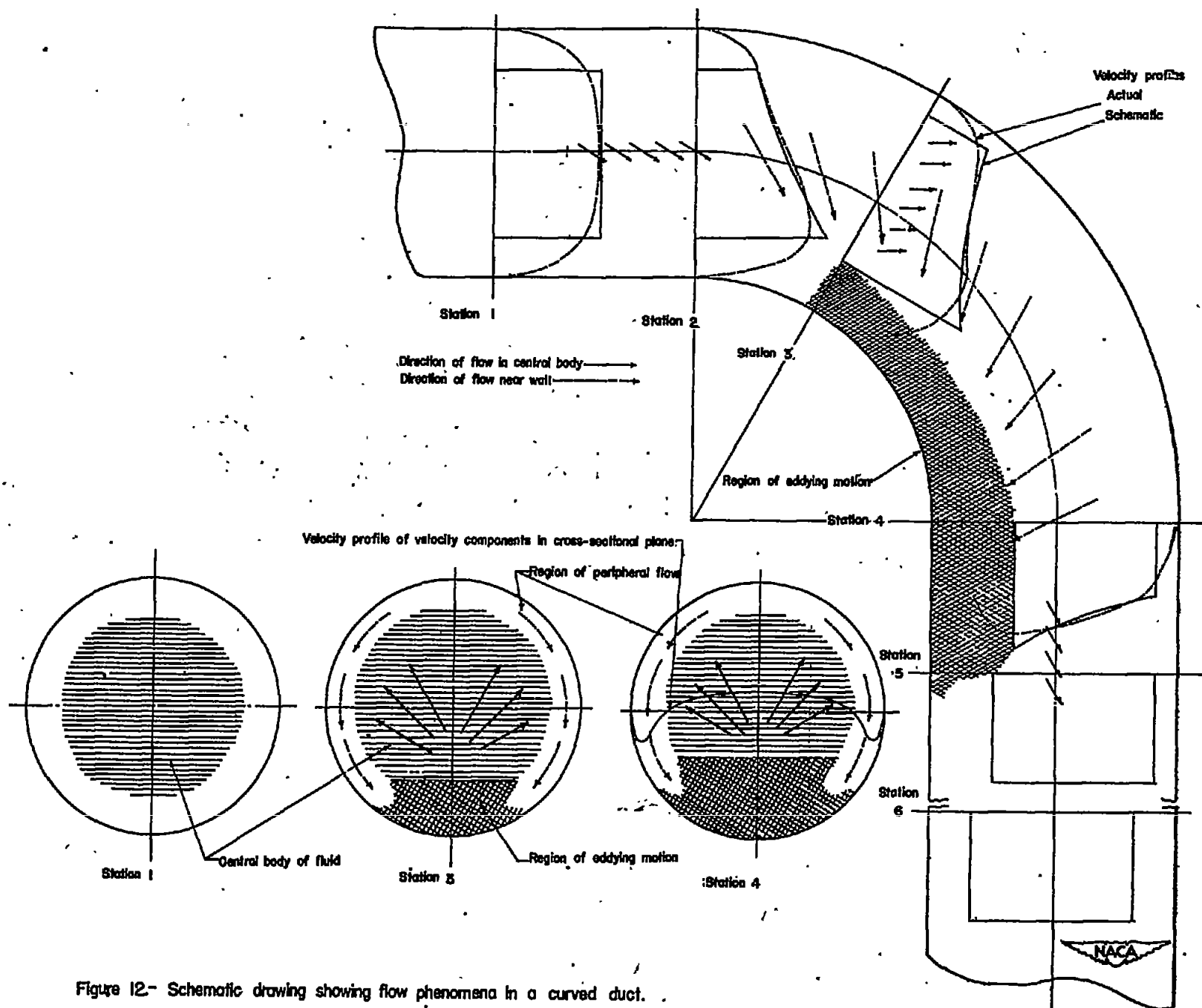


Figure 12.- Schematic drawing showing flow phenomena in a curved duct.

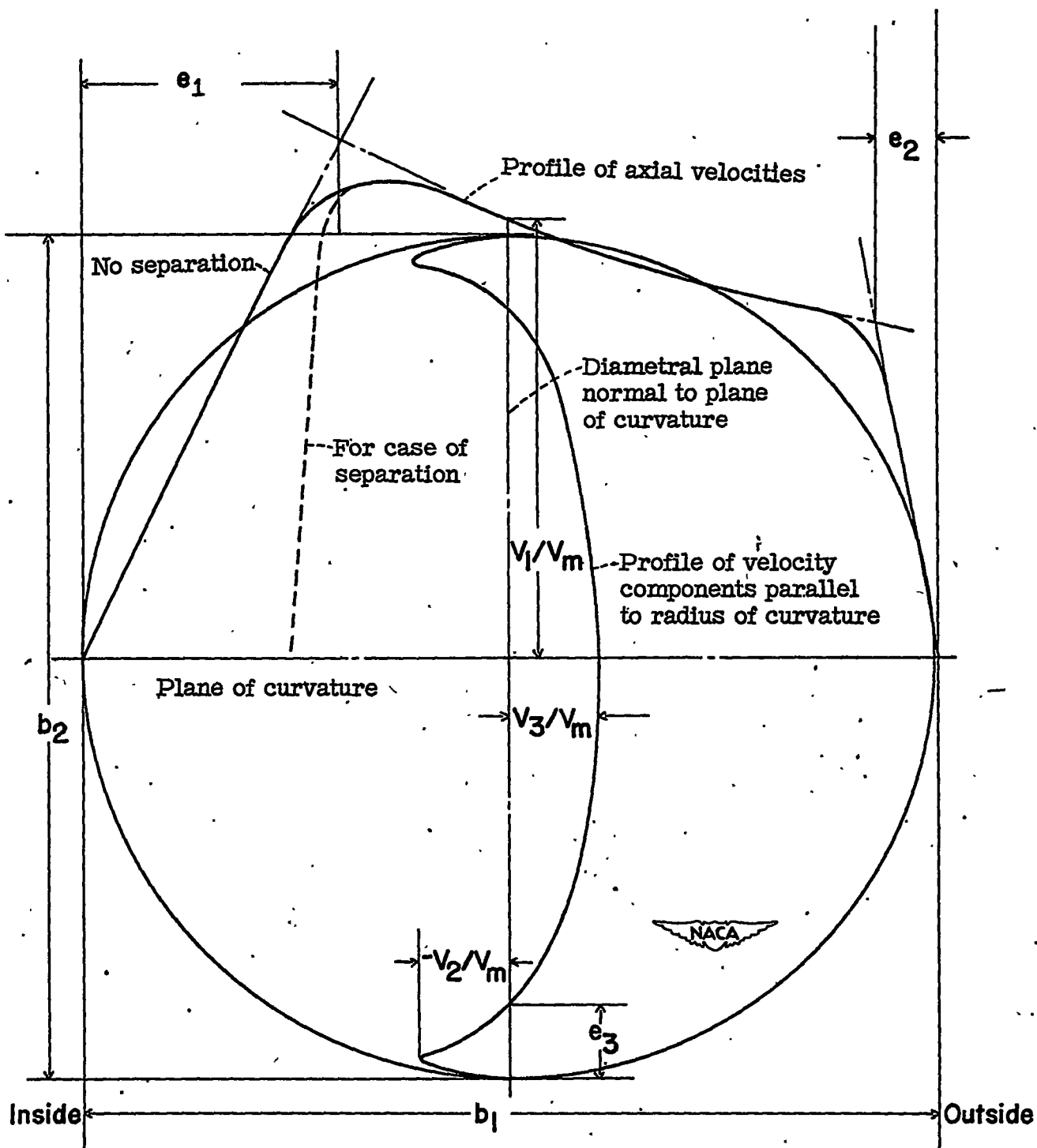


Figure 13.- Diagram and notations defining velocity distribution in curved ducts. For circular cross section $b_1 = b_2 = d$.

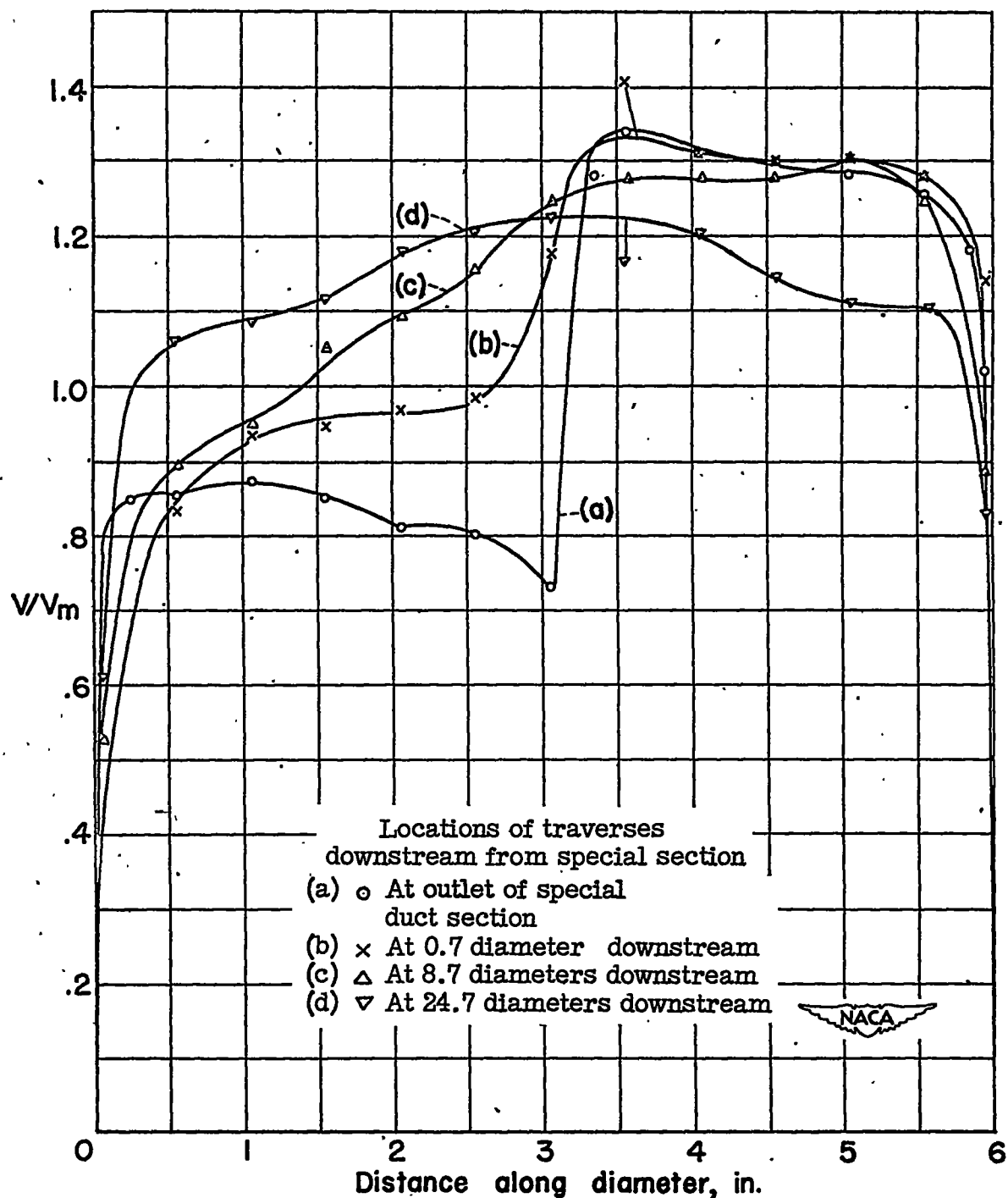


Figure 14.- Decay of a velocity continuity produced by half-screened 6-inch-diameter duct section (fig. 3) at various distances downstream.

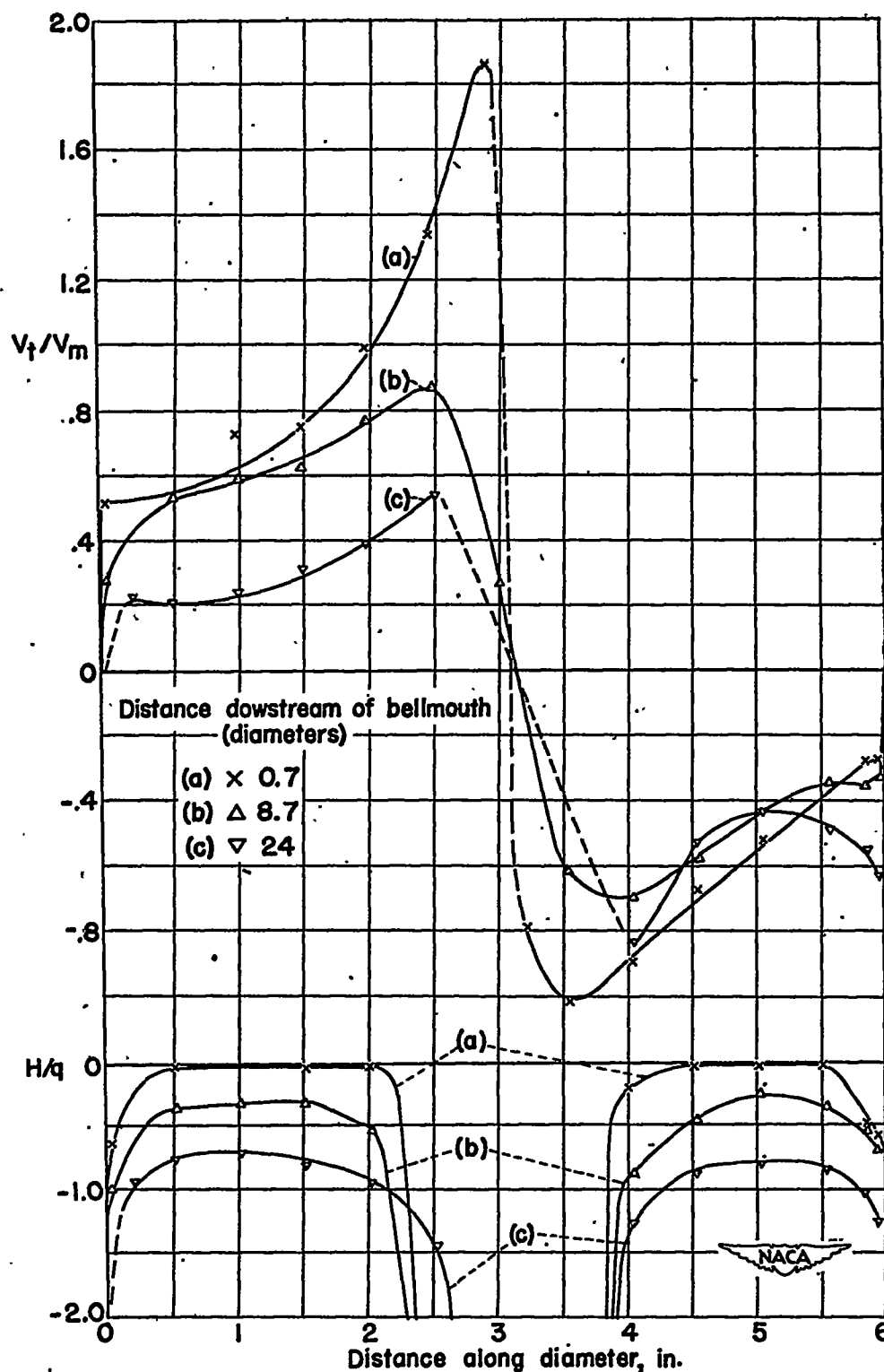


Figure 15.- Decay of a vortex in a straight duct of 6-inch-diameter circular cross section. $R = 0.304 \times 10^{-6}$.

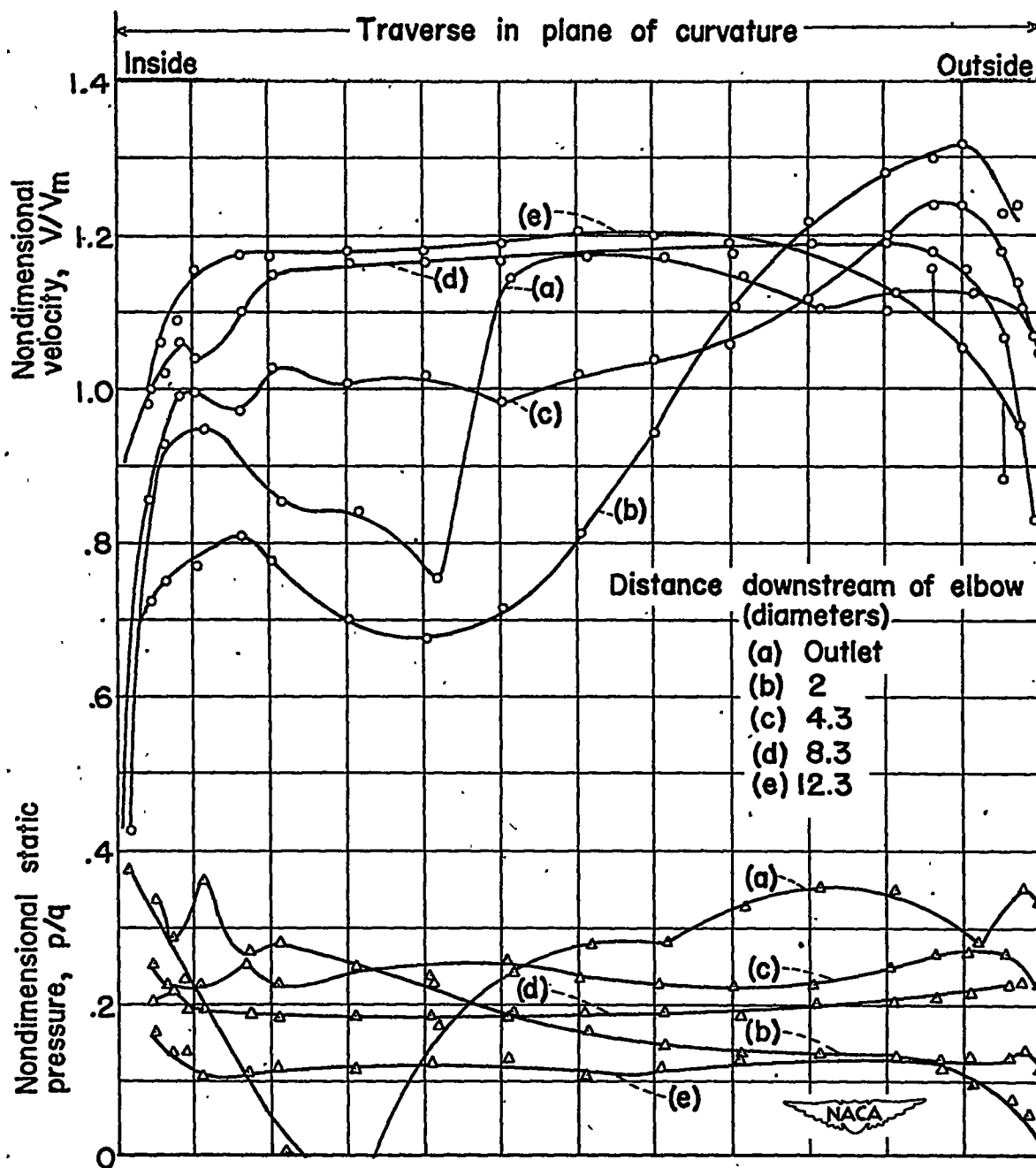


Figure 16.- Velocity and static-pressure traverse in plane of curvature at various distances downstream of a 90° elbow of circular cross section 6 inches in diameter. $\frac{r}{b} = 1.5$; $R = 0.304 \times 10^6$.

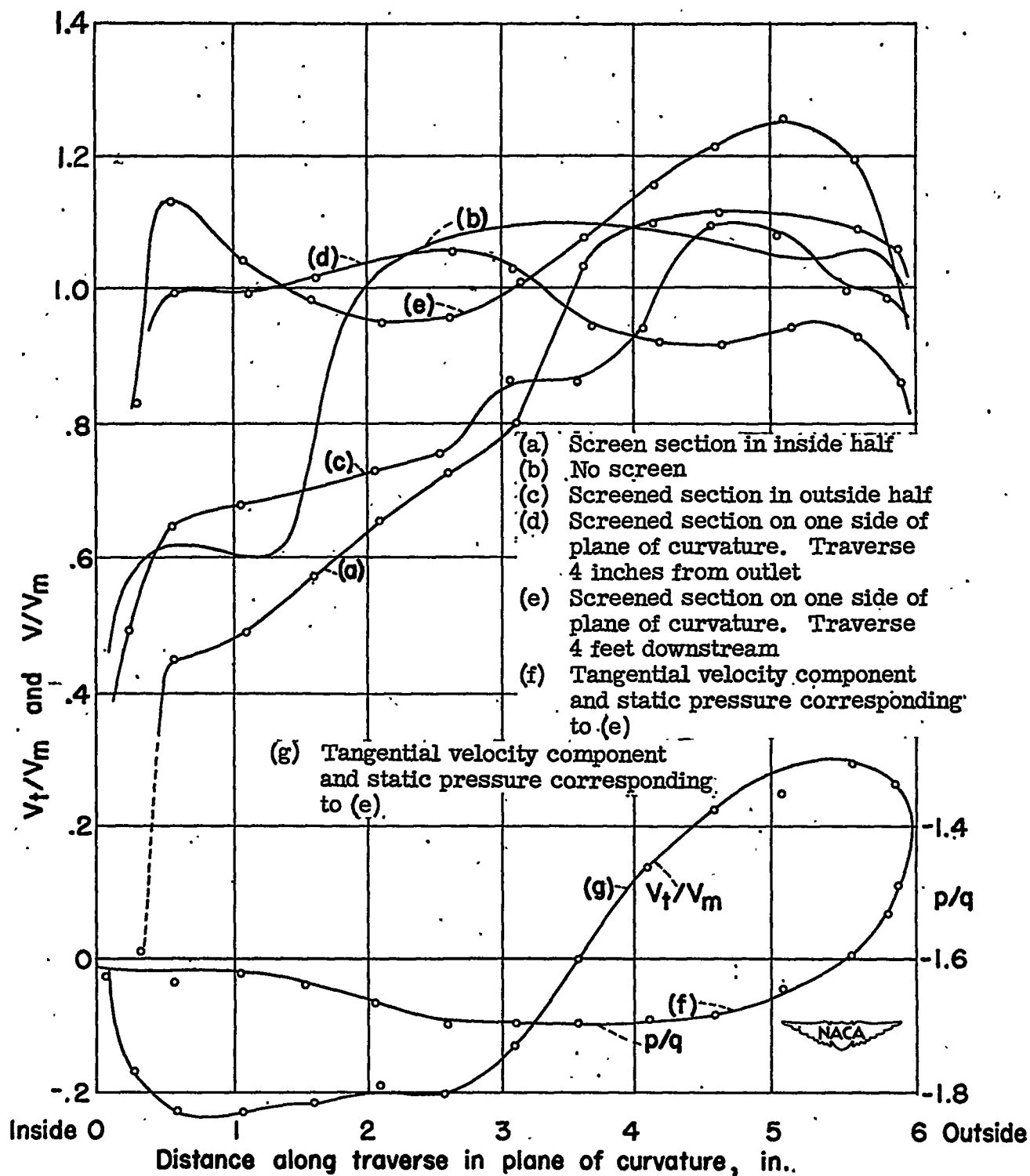


Figure 17.- Effect of unsymmetries upstream upon velocity distribution in a 6-inch-diameter, 90° elbow. $\frac{r}{b_1} = 1.5$ at $R = 0.3 \times 10^6$.